Radiology

ORIGINAL RESEARCH • GASTROINTESTINAL IMAGING

Association between Liver MRI Proton Density Fat Fraction and Liver Disease Risk

Tianyi Xia, MD • Mulong Du, PhD • Huiqin Li, MM • Yuancheng Wang, MD • Junhao Zha, MD • Tong Wu, MD • Shenghong Ju, MD, PhD

From the Jiangsu Key Laboratory of Molecular and Functional Imaging, Department of Radiology, Zhongda Hospital, School of Medicine, Southeast University, 87 Ding Jia Qiao Road, Nanjing 210009, China (T.X., Y.W., J.Z., T.W., S.J.); and Department of Biostatistics, Center for Global Health, School of Public Health, Nanjing Medical University, Nanjing, China (M.D., H.L.). Received April 19, 2023; revision requested June 27; revision received August 24; accepted August 31. **Address correspondence to** S.H.J. (email: *jsh@seu.edu.cn*).

Supported by the National Natural Science Foundation of China (NSFC, No. 81830053) and National Key Research and Development Program of China (2021YFF0501504).

Conflicts of interest are listed at the end of this article.

See also the editorials by Reeder and Starekova and Monsell in this issue.

Radiology 2023; 309(1):e231007 • https://doi.org/10.1148/radiol.231007 • Content codes: GI MR RS

Background: A better understanding of the association between liver MRI proton density fat fraction (PDFF) and liver diseases might support the clinical implementation of MRI PDFF.

Purpose: To quantify the genetically predicted causal effect of liver MRI PDFF on liver disease risk.

Materials and Methods: This population-based prospective observational study used summary-level data mainly from the UK Biobank and FinnGen. Mendelian randomization analysis was conducted using the inverse variance–weighted method to explore the causal association between genetically predicted liver MRI PDFF and liver disease risk with Bonferroni correction. The individual-level data were downloaded between August and December 2020 from the UK Biobank. Logistic regression analysis was performed to validate the association between liver MRI PDFF polygenic risk score and liver disease risk. Mediation analyses were performed using multivariable mendelian randomization.

Results: Summary-level and individual-level data were obtained from 32 858 participants and 378 436 participants (mean age, 57 years ± 8 [SD]; 203 108 female participants), respectively. Genetically predicted high liver MRI PDFF was associated with increased risks of malignant liver neoplasm (odds ratio [OR], 4.5; $P < .001$), alcoholic liver disease (OR, 1.9; $P < .001$), fibrosis and cirrhosis of the liver (OR, 3.0; $P < .004$), fibrosis of the liver (OR, 3.6; $P = .002$), cirrhosis of the liver (OR, 3.8; $P < .001$), nonalcoholic steatohepatitis (OR, 7.7; $P < .001$), and nonalcoholic fatty liver disease (NAFLD) (OR, 4.4; $P < .001$). Individual-level evidence supported these associations after grouping participants based on liver MRI PDFF polygenic risk score (all $P < .004$). The mediation analysis indicated that genetically predicted high-density lipoprotein cholesterol, type 2 diabetes mellitus, and waist-to-hip ratio (mediation effects, 25.1%–46.3%) were related to the occurrence of fibrosis and cirrhosis of the liver, cirrhosis of the liver, and NAFLD at liver MRI PDFF (all $P < .05$).

Conclusion: This study provided evidence of the association between genetically predicted liver MRI PDFF and liver health.

© RSNA, 2023

Supplemental material is available for this article.

An earlier incorrect version appeared online. This article was corrected on October 31, 2023.

Hepatic steatosis is characterized by abnormal accumulation of lipids, especially triglycerides, in hepatocytes cytoplasm (1). Hepatic steatosis is one of the histologic characteristics of nonalcoholic fatty liver disease (NAFLD) and is the leading cause of chronic liver disease globally (2). Hepatic steatosis is known to progress into more serious liver diseases, including nonalcoholic steatohepatitis (NASH), liver fibrosis and cirrhosis, and even cancer (3).

Due to recent advancements in imaging technology, liver fat content can be measured noninvasively and quantitatively. Among various imaging modalities, MRI proton density fat fraction (PDFF) has demonstrated the highest diagnostic precision and has been used extensively in early-phase clinical trials for NASH to assess treatment effectiveness (4). Liver MRI PDFF provides valuable information regarding triglyceride accumulation within hepatic tissue. Importantly, reductions in MRI PDFF have shown a strong correlation with improvements in hepatic steatosis and other histologic features like fibrosis, ballooning degeneration, and lobular inflammation (5,6).

The UK Biobank, which contains genetic and health-related information from over 500 000 volunteers in Scotland, Northern Ireland, Wales, and England, contains MRI and other medical imaging data for several organs (7). In hepatology, liver MRI functional phenotypes such as liver iron and MRI PDFF have demonstrated potential clinical value (8–10). Mendelian randomization analysis, an approach that uses instrumental variables and summary-level data, helps determine causal effects while minimizing confounding and reverse causality biases (11). A recent study (12) showed a causal association between liver MRI PDFF and type 2 diabetes mellitus.

Epidemiologic studies have highlighted the importance of risk factors such as serum lipids, body composition, and insulin resistance in the progression of NAFLD, which also may impact MRI PDFF (13). It is relevant to investigate

This copy is for personal use only. To order copies, contact *reprints@rsna.org*

Abbreviations

NAFLD = nonalcoholic fatty liver disease, NASH = nonalcoholic steatohepatitis, OR = odds ratio, PDFF = proton density fat fraction, PRS = polygenic risk score, SNP = single nucleotide polymorphism

Summary

Liver MRI proton density fat fraction demonstrated a causal association with liver disease risk and may serve as a mediator of metabolic phenotypes.

Key Results

- Liver MRI proton density fat fraction (PDFF) was associated with increased risks of malignant liver neoplasm, alcoholic liver disease, fibrosis and cirrhosis of liver, fibrosis of liver, cirrhosis of liver, nonalcoholic steatohepatitis, and nonalcoholic fatty liver disease (NAFLD) ($P < .004$).
- High-density lipoprotein cholesterol, type 2 diabetes mellitus, and waist-to-hip ratio (mediation effects, 25.1%–46.3%) were related to fibrosis and cirrhosis of liver, cirrhosis of liver, and NAFLD at liver MRI PDFF ($P < .05$).

the effects of fat metabolism because there are intricate metabolic and endocrine links between other fat-related factors and liver health. We proposed a hypothesis that likens the relationship between the risk factors, liver MRI PDFF, and liver disease to that of fertilizers, soils, and vegetation; liver MRI PDFF may serve as a crucial intermediate link. Yet, investigations of such causal associations are lacking.

In this study, a two-sample mendelian randomization framework was systematically performed to investigate the causal association between liver MRI PDFF and liver disease risk. A two-step mendelian randomization and a multivariable mendelian randomization analyses were also conducted to investigate the mediating pathways from potential risk factors of liver disease by using liver MRI PDFF because these pathways may be crucial in the prevention and treatment of liver diseases.

Materials and Methods

Data Sources and Study Participants

For summary-level data, analysis was performed using publicly available summary statistics. The inclusion and exclusion criteria remained consistent with previous publications; the study was approved by the institutional review boards and written informed consent was obtained from all participants (10,14). This study adheres to the Strengthening the Reporting of Observational Studies in Epidemiology using Mendelian Randomization guideline (15).

Descriptions of all phenotypes are in Table 1 and Appendix S1. All summary-level data are from individuals with European ancestry without a known sample overlap. The 11 potential risk factors for liver MRI PDFF can be summarized as insulin resistance, body composition, and serum lipids. The liver MRI PDFF phenotype was based on 32 859 individuals of European ancestry in the UK Biobank (10). The summary-level data from 12 liver diseases were collected from the FinnGen (seventh release), a database of genotype and health registry data of volunteers in Finland, including 309 154 individuals of European ancestry. Liver diseases were defined as binary outcomes from the 10th edition of the international classification of diseases codes (Fig 1).

At individual-level data (application number 45611), 502 528 individuals between the ages of 40 and 69 years were recruited in the prospective population-based UK Biobank. A total of 378 436 participants were analyzed after the following quality control procedures were implemented: excluding individuals with sex discrepancies; excluding outliers for genotype missingness or excess heterozygosity; retaining unrelated participants; restricting to "White British" individuals of European ancestry; removing individuals who refused to participate in the program; and excluding the individuals without liver diseases information (Fig S1). The remaining 378 436 participants were used for developing the liver MRI PDFF–weighted polygenic risk score (PRS) (Appendix S2). We summed 10 liver MRI PDFF–associated single nucleotide polymorphisms (SNPs), weighted by corresponding effect sizes (Table S1). Between August 2020 and December 2020, individual data were downloaded and underwent quality control. The previous data set was used to investigate the association between circulating vitamin E and 10 common cancers, unrelated to the current study (16). A current analysis of the individual data was conducted between October 2022 and April 2023.

Mendelian Randomization Study Design

Study pipeline.—The following three fundamental presumptions were considered when conducting Mendelian randomization: that the genetic variants are strongly associated with the exposure, that the genetic variants are not associated with any potential confounder of the exposure-outcome association, and that the variants do not affect outcome independently of exposure. Figure 1 shows the analysis flowchart, including the analysis of summary-level and individual-level data.

Selection of genetic instrumental variables.—SNPs that reached genome-wide significance of $P < 5 \times 10^{-8}$ were selected as instrumental variables. A strict cut-off of linkage disequilibrium ($r^2 < 0.001$) within a window of 10 000 kb was implemented for independent SNPs. The effects of SNPs on exposure and outcome were then harmonized, and palindromic and outlier SNPs ($P < .05$) were removed by the mendelian randomization-pleiotropy residual sum and outlier method. The remaining SNPs were used to perform mendelian randomization analysis (Appendix S2).

Statistical Analysis

The inverse variance–weighted method with a random-effects model was used as the primary analysis of univariable mendelian randomization, and weighted median and mendelian randomization–Egger methods were used as supplements. The Cochrane Q statistic was used to assess the heterogeneity ($P < .05$). The mendelian randomization–Egger method was used to assess potential pleiotropy ($P < .05$). If heterogeneity existed, a random-effects inverse variance–weighted mendelian randomization analysis was used for consideration of

Table 1: Characteristics of Genome-wide Association Studies of Phenotypes Included

Phenotype	Unit	Cohort	Sample Size	PMID
Image phenotype				34128465
Liver MRI PDFF	SD	UK Biobank	32 858	
Serum lipids		GLGC		24097068
Total cholesterol	SD	…	94 595	…
Triglycerides	SD	…	94 595	…
HDL-C	SD	…	94 595	…
LDL-C	SD	…	94 595	…
Liver disease (code)		FinnGen		NA
C22: Malignant liver neoplasm	LogOR	…	309 154	…
D13.4 or D13.5: Benign liver neoplasm	LogOR	…	309 154	…
K70: alcoholic liver disease	LogOR	…	303 167	…
K71: Toxic liver disease	LogOR	…	301 301	…
K72: Hepatic failure	LogOR	…	301 737	…
K73: Chronic hepatitis	LogOR	…	301 713	…
K74: Fibrosis and cirrhosis of liver	LogOR	…	302 376	…
K75: Other inflammatory liver diseases	LogOR	…	302 424	…
K74.0: Fibrosis of liver	LogOR	…	306 256	…
K74.6: Cirrhosis of liver	LogOR	…	306 971	…
K75.8: NASH	LogOR	…	309 154	…
K76.0: NAFLD	LogOR	…	309 154	…
Body composition				
BMI	SD	GIANT	322 154	25673413
Waist-to-hip ratio	SD	GIANT	224 459	25673412
Body fat percentage	SD	NA	65 831	26833246
Insulin resistance				
Fasting glucose	SD	MAGIC	58 074	22581228
Fasting insulin	SD	MAGIC	51 750	22581228
HbA1C	SD	MAGIC	46 368	20858683
T2DM	LogOR	DIAGRAM	69 033	22885922

Note.—Data are numbers of participants. The entire study population was of European ancestry. Codes are from 10th edition of the *International Classification of Diseases*. BMI = body mass index, DIAGRAM = Diabetes Genetics Replication and Meta-analysis, GIANT = Genetic Investigation of Anthropometric Traits, GLGC = Global Lipids Genetics Consortium, HbA1C = hemoglobin A1C, HDL-C = high-density lipoprotein cholesterol, LDL-C = low-density lipoprotein cholesterol, LogOR = the logarithm of odds ratio, MAGIC = Meta-analyses of Glucose and Insulin-Related Traits Consortium, NA = not available, NAFLD = nonalcoholic fatty liver disease, NASH = nonalcoholic steatohepatitis, PDFF = proton density fat fraction, PMID = PubMed Unique Identifier, T2DM = type 2 diabetes mellitus.

potential heterogeneity among multiple different SNPs. Additionally, a leave-one-out analysis, bidirectional mendelian randomization analysis, and Steiger direction test for statistical significance were performed to evaluate influential outliers and determine the direction of a causal effect. Bonferroni correction was used to adjust for multiple testing of liver MRI PDFF and liver disease with $P < .004$ (.05/12) indicating statistical significance, and $P < .05$ was regarded as indicating nominal significance in two-sample mendelian randomization analysis. The genetic collection was examined by linkage disequilibrium score regression (17). The mRnd *(https://shiny.cnsgenomics.com/mRnd/)* was used to calculate the statistical power (18). The association of the PRS of liver MRI PDFF with liver disease risk was evaluated by logistic regression with adjustment for sex, age, smoking status, drinking status, and the first 10 principal components. Bonferroni correction was used to adjust for multiple testing of PRS and liver disease, with $P < .05/12$ (.004).

Multivariable mendelian randomization with the inverse variance–weighted method was performed to estimate the independent effect of liver MRI PDFF on each outcome after adjusting for each risk factor. This was performed only when the pathway of mediation (the univariable mendelian randomization results of exposure mediator and mediator outcome) was statistically significant ($P < .05$).

The mediated effect was calculated after the product of the coefficient method. Standard errors were estimated with the Δ method, in which effect estimates were calculated from univariable mendelian randomization (exposure outcome, exposure mediator) or multivariable mendelian randomization (mediator outcome). The Sobel test was used to evaluate the proportion of the mediation effect ($P < .05$). The proportion of the effect mediated was calculated by dividing the indirect effect by the total effect. The mendelian randomization analysis was performed using R packages (TwoSampleMR and ldscr; R Project for Statistical Computing). All statistical analyses were

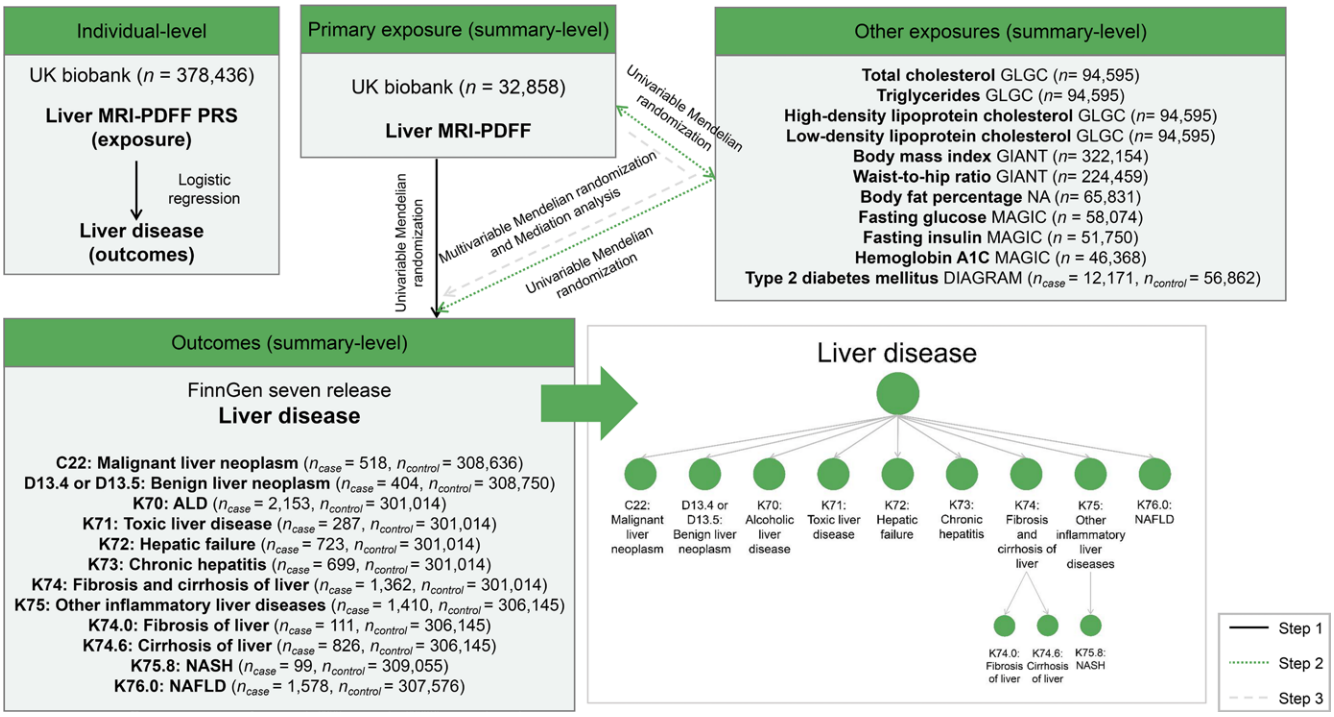

Figure 1: Study data and analysis flowchart. Genome-wide association study summary-level data were acquired from the UK Biobank, FinnGen, and other consortiums. For individual-level data, liver MRI proton density fat fraction (PDFF) polygenic risk score (PRS) was constructed as the exposure from the UK Biobank. For summary-level data, mendelian randomization analysis was conducted for the exposure of liver MRI PDFF and the outcomes of liver diseases (bottom right). The lines represent the steps of the study. In the summary-level outcomes (lower left) and the resulting liver disease (lower right), data associated with the disease are codes from the 10th edition of the *International Classification of Diseases*. ALD = alcoholic liver disease, DIAGRAM = Diabetes Genetics Replication and Meta-analysis, GIANT = Genetic Investigation of Anthropometric Traits, GLGC = Global Lipids Genetics Consortium, MAGIC = Meta-analyses of Glucose and Insulin-Related Traits Consortium, NA = not available, NAFLD = nonalcoholic fatty liver disease, NASH = nonalcoholic steatohepatitis, n_{case} = number of cases, $n_{control}$ = number of control cases.

performed in by using statistical software (R version 4.2.2; *https://www.r-project.org/*).

Results

Relationship between Liver MRI PDFF and Liver Disease Risk

The number of SNPs of liver MRI PDFF used for univariable mendelian randomization ranged from eight to 10, with *F* statistics ranging from 57 to 148. Univariable mendelian randomization analysis showed a causal association with a higher odds ratio (OR) of genetically predicted liver MRI PDFF in several liver diseases, including malignant liver neoplasm (OR, 4.5; 95% CI: 2.7, 7.4; $P < .001$), alcoholic liver disease (OR, 1.9; 95% CI: 1.4, 2.7; $P < .001$), fibrosis and cirrhosis of the liver (OR, 3.0; 95% CI: 2.3, 4.0; $P < .001$), fibrosis of the liver (OR, 3.6; 95% CI: 1.6, 8.3; $P = .002$), cirrhosis of the liver (OR, 3.8; 95% CI: 2.4, 5.9; $P < .001$), NASH (OR, 7.7; 95% CI: 3.7, 15.7; $P < .001$), and NAFLD (OR, 4.4; 95% CI: 2.6, 7.5; $P < .001$) (Table 2, Fig 2).

The weighted median and mendelian randomization–Egger methods provided consistent findings with the relationships. The Cochran Q statistic indicated no evidence of heterogeneity across instrument effects (all $P > .05$). No evidence of directional pleiotropy was identified by mendelian randomization–Egger intercept analysis (all $P > .05$). The associations between liver MRI PDFF and mentioned liver disease risk and leave-one-out analysis are in Figures S2 and S3. There were genetic correlations between liver MRI PDFF and outcome phenotypes of alcoholic liver disease (correlation coefficient, 0.29; $P = .02$) and NAFLD (correlation coefficient, 0.74; $P < .001$) (Table S2). The statistical powers for alcoholic liver disease and fibrosis of the liver were only 61% and 50%, with other phenotypes ranging from 99% to 100% (Table S3).

Moreover, the inverse variance–weighted results indicated nominally significant associations between liver MRI PDFF and the effect of chronic hepatitis (OR, 1.7; 95% CI: 1.2, 2.6; $P = .007$) and other inflammatory liver diseases (OR, 1.3; 95% CI: 1.03, 1.6; $P = .03$). There was no evidence of an association between liver MRI PDFF and the effect of benign liver neoplasm (OR, 1.2; 95% CI: 0.8, 1.9; $P = .35$), toxic liver disease (OR, 1.3; 95% CI: 0.4, 4.2; $P = .34$), and hepatic failure (OR, 1.7; 95% CI: 0.8, 3.4; $P = .14$).

In the validation stage at the individual-level data, data of 378 436 participants (mean age, 57 years ± 8 [SD]; 203 108 women) were obtained. The results of logistic regression based on liver MRI PDFF indicated that PRS of MRI PDFF was significantly associated with malignant liver neoplasm (OR, 3.7; 95% CI: 2.8, 5.0), alcoholic liver disease (OR, 3.8; 95% CI: 3.0, 4.7), hepatic failure (OR, 2.8; 95% CI: 2.1, 3.9), fibrosis and cirrhosis of the liver (OR, 4.2; 95% CI: 3.4, 5.1), other inflammatory liver diseases (OR, 2.8;

Table 2: Univariable Mendelian Randomization Results for the Relationship between Liver MRI Proton Density Fat Fraction and Liver Disease

Parameter	No. of SNPs	*F* Statistic	Odds Ratio	*P* Value	Het-*P* Value	Ple-*P* Value
Malignant liver neoplasm (C22)	8	106				
IVW			4.5 (2.7, 7.4)	<.001	.60	
Weighted median			5.4 (3.0, 9.5)	<.001		
MR-Egger			6.5 (3.1, 13.9)	.003	.52	.25
Benign liver neoplasm (D13.4 or D13.5)	10	148				
IVW			1.2 (0.8, 1.9)	.35	.84	
Weighted median			1.1 (0.7, 1.9)	.67		
MR-Egger			1.4 (0.7, 2.6)	.38	.89	.69
Alcoholic liver disease (K70)	8	106				
IVW			1.9 (1.4, 2.7)	<.001	.13	
Weighted median			1.8 (1.3, 2.5)	<.001		
MR-Egger			1.7 (0.97, 2.8)	.12	.15	.51
Toxic liver disease (K71)	8	57				
IVW			1.3 (0.4, 4.2)	.34	.08	
Weighted median			1.1 (0.4, 2.9)	.79		
MR-Egger			0.5 (0.1, 3.3)	.66	.045	.26
Hepatic failure (K72)	8	57				
IVW			1.7 (0.8, 3.4)	.14	.04	
Weighted median			1.7 (0.9, 3.2)	.07		
MR-Egger			1.7 (0.5, 5.9)	.41	.06	.94
Chronic hepatitis (K73)	10	148				
IVW			1.7 (1.2, 2.6)	.007	.12	
Weighted median			1.8 (1.2, 2.7)	.005		
MR-Egger			1.4 (0.8, 2.7)	.29	.14	.48
Fibrosis and cirrhosis of liver (K74)	9	105				
IVW			3.0 (2.3, 4.0)	<.001	.28	
Weighted median			3.0 (2.2, 4.2)	<.001		
MR-Egger			2.7 (1.8, 4.2)	.003	.33	.51
Other inflammatory liver diseases (K75)	10	148				
IVW			1.3 (1.03, 1.6)	.03	.48	
Weighted median			1.2 (0.9, 1.7)	.19		
MR-Egger			1.2 (0.9, 1.8)	.28	.57	.74
Fibrosis of liver (K74.0)	10	148				
IVW			3.6 (1.6, 8.3)	.002	.27	
Weighted median			4.2 (1.5, 11.3)	.006		
MR-Egger			2.3 (0.6, 8.9)	.25	.30	.44
Cirrhosis of liver (K74.6)	8	106				
IVW			3.8 (2.4, 5.9)	<.001	.37	
Weighted median			3.2 (2.0, 5.2)	<.001		
MR-Egger			2.7 (1.4, 5.2)	.03	.30	.24
NASH (K75.8)	10	148				
IVW			7.7 (3.7, 15.7)	<.001	.41	
Weighted median			11.1 (4.3, 28.8)	<.001		
MR-Egger			6.9 (2.2, 22.0)	.01	.51	.83
NAFLD (K76.0)	8	57				
IVW			4.4 (2.6, 7.5)	<.001	.08	
Weighted median			4.4 (2.8, 6.9)	<.001		
MR-Egger			2.5 (1.2, 5.0)	.043	.006	.08

Note.—Data in parentheses are 95% CIs. Het-*P* indicates the *P* value of Cochrane *Q* value in the heterogeneity test, and Ple-*P* indicates the *P* value of the mendelian randomization–Egger (MR-Egger) intercept. The codes in parentheses after the disease are from the 10th edition of the *International Classification of Diseases*. IVW = inverse variance–weighted, NAFLD = nonalcoholic fatty liver disease, NASH = nonalcoholic steatohepatitis, SNP = single nucleotide polymorphism.

95% CI: 2.2, 3.5), fibrosis of the liver (OR, 3.2; 95% CI: 1.8, 5.4), cirrhosis of the liver (OR, 5.4; 95% CI: 4.3, 6.8), NASH (OR, 9.3; 95% CI: 6.5, 13.3), and NAFLD (OR, 3.6; 95% CI: 3.1, 4.0) (all $P < .004$) (Table 3). According to cutoff values of 10% and 90%, PRS was divided into three groups: low PRS, intermediate PRS, and high PRS. The risk of these liver diseases also increased with a higher PRS of MRI PDFF (Fig 3, Table S4).

Direction and Effect of Potential Risk Factors

Evidence for a causal effect of body mass index ($\beta = 0.16$; $P < .001$), waist-to-hip ratio ($\beta = 0.27$; $P < .001$), high-density lipoprotein cholesterol ($\beta = -0.05$; $P = .03$), low-density lipoprotein cholesterol ($\beta = -0.05$; $P = .02$), and type 2 diabetes mellitus ($\beta = 0.08$; $P < .001$) on liver MRI PDFF images was detected without pleiotropy (Table S5). The Cochran Q statistic found heterogeneity across instrument effects for body mass index ($P = .01$) and high-density lipoprotein cholesterol ($P < .001$).

In bidirectional mendelian randomization analysis, evidence for a causal effect of liver MRI PDFF on low-density lipoprotein cholesterol ($\beta = 0.46$; $P < .001$) was detected without heterogeneity and pleiotropy (Table S6). Stegier direction test indicated the directions between risk factors and liver MRI PDFF (Table S7). Because of the bidirectional causality and pleiotropy, low-density lipoprotein cholesterol and triglycerides were not analyzed subsequently.

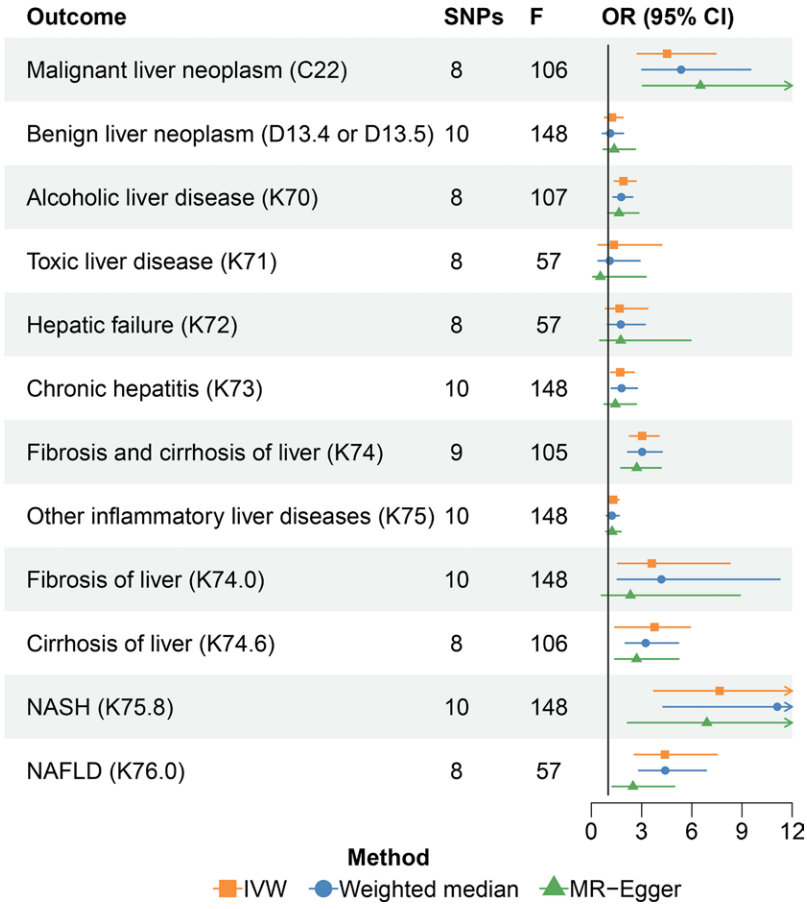

Figure 2: Forest plot shows the association between liver MRI PDFF and liver disease by different mendelian randomization methods. Odds ratios are presented, with 95% CIs. The codes in parentheses after the disease are defined from the 10th edition of the *International Classification of Diseases*. IVW = inverse variance weighted, NAFLD = nonalcoholic fatty liver disease, NASH = nonalcoholic steatohepatitis, OR = odds ratio, SNP = single nucleotide polymorphism.

The inverse variance–weighted results for associations between potential risk factors and liver diseases showed a causal association between body mass index and NAFLD (OR, 1.8; 95% CI: 1.3, 2.6; $P = .002$); waist-to-hip ratio and fibrosis and cirrhosis of the liver (OR, 2.1; 95% CI: 1.03, 4.2; $P = .04$), fibrosis of the liver (OR, 19.8; 95% CI: 1.7, 22.8; $P = .02$), cirrhosis of the liver (OR, 3.2; 95% CI: 1.4, 7.2; $P = .006$), NASH (OR, 15.7; 95% CI: 1.4, 178.9; $P = .03$), and NAFLD (OR, 2.8; 95% CI: 1.5, 5.5; $P = .002$); high-density lipoprotein cholesterol and NAFLD (OR, 0.7; 95% CI: 0.6, 0.9; $P = .01$); and type 2 diabetes mellitus and NAFLD (OR, 1.3; 95% CI: 1.1, 1.5; $P = .004$), all without heterogeneity and pleiotropy (Table S8).

Identifying the Causal Pathway by Liver MRI PDFF

After adjusting for waist-to-hip ratio, multivariable mendelian randomization analysis estimated that liver MRI PDFF was associated with fibrosis and cirrhosis of the liver (OR, 2.9; 95% CI: 1.9, 4.3; $P < .001$), cirrhosis of the liver (OR, 3.4; 95% CI: 2.2, 5.5; $P < .001$), and NAFLD (OR, 4.4; 95% CI: 2.1, 9.4; $P < .001$). Liver MRI PDFF was associated with NALFD after adjusting for high-density lipoprotein cholesterol (OR, 4.3; 95% CI: 2.3, 7.8; $P < .001$) and type 2 diabetes mellitus (OR, 4.4; 95% CI: 2.1, 9.2; $P < .001$) (Table S9).

The indirect effect of potential risk factors (type 2 diabetes mellitus, waist-to-hip ratio, and high-density lipoprotein cholesterol) on liver diseases (fibrosis and cirrhosis of liver, cirrhosis of liver, and NAFLD) with liver MRI PDFF was also assessed (Table 4), showing 25.1% mediation effects of high-density lipoprotein cholesterol at liver MRI PDFF on NAFLD ($P = .046$) and 46.3% mediation effects of type 2 diabetes mellitus on NAFLD ($P = .008$). Moreover, waist-to-hip ratio (28.7%–38.4% mediation effects) was causally related to fibrosis and cirrhosis of the liver, cirrhosis of the liver, and NAFLD via liver MRI PDFF (all $P < .05$) (Fig 4). Figure 5 shows the causal associations and mediation role of liver MRI PDFF in the pathway from potential risk factors to liver disease.

Discussion

Mendelian randomization analysis on a broad scale was used to fully pinpoint the relationship between liver MRI proton density fat fraction (PDFF) and liver disease risk. We found evidence of a significant positive genetic correlation between liver MRI PDFF and several liver disease risks (eg, malignant liver neoplasm, alcoholic liver disease, fibrosis and cirrhosis of the liver, nonalcoholic fatty liver disease, and nonalcoholic steatohepatitis; all $P < .004$

Table 3: Results for the Relationship between Liver MRI Proton Density Fat Fraction Polygenic Risk Score and Liver Disease in UK Biobank

Liver Disease	No. of Cases	Odds Ratio*	*P* Value
Malignant liver neoplasm (C22)	816	3.7 (2.8, 5.0)	<.001
Benign liver neoplasm (D13.4 or D13.5)	141	1.4 (0.6, 2.9)	.41
Alcoholic liver disease (K70)	1381	3.8 (3.0, 4.7)	<.001
Toxic liver disease (K71)	109	1.9 (0.8, 4.5)	.14
Hepatic failure (K72)	775	2.8 (2.1, 3.9)	<.001
Chronic hepatitis (K73)	167	0.8 (0.4, 1.7)	.63
Fibrosis and cirrhosis of liver (K74)	1747	4.2 (3.4, 5.1)	<.001
Other inflammatory liver diseases (K75)	1330	2.8 (2.2, 3.5)	<.001
Fibrosis of liver (K74.0)	243	3.2 (1.8, 5.4)	<.001
Cirrhosis of liver (K74.6)	1271	5.4 (4.3, 6.8)	<.001
NASH (K75.8)	481	9.3 (6.5, 13.3)	<.001
NAFLD (K76.0)	4641	3.6 (3.1, 4.0)	<.001

Note.— There are 378 436 participants total. The codes in parentheses after the disease are defined from the 10th edition of the *International Classification of Diseases*. NAFLD = nonalcoholic fatty liver disease, NASH = nonalcoholic steatohepatitis.
* Data in parentheses are 95% CIs. Odds ratios are adjusted for sex, age, study centers, smoking status, drinking status, and first 10 principal components, when appropriate.

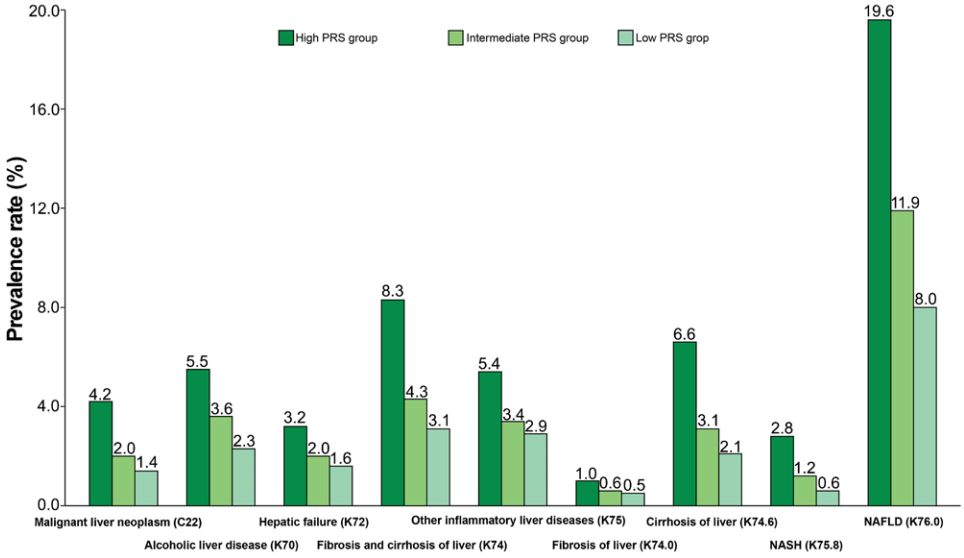

Figure 3: Vertical bar plot of associations between the liver MRI proton density fat fraction polygenic risk score (PRS) groups and liver disease prevalence. The codes in parentheses after the disease are defined from the 10th edition of the *International Classification of Diseases*. Three PRS groups were formed by PRS cutoff values of 10% and 90%. The unit of the prevalence is permillages. NAFLD = nonalcoholic fatty liver disease, NASH = nonalcoholic steatohepatitis, PRS = polygenic risk score.

in summary-level and individual-level data). Further mediation analysis suggested that liver MRI PDFF may serve as a possible "transfer station" between the etiologic factors (high-density lipoprotein cholesterol, type 2 diabetes mellitus, and waist-to-hip ratio) and mentioned liver diseases (all $P < .005$). These findings are important for better prevention of liver health by MRI PDFF dynamic monitoring.

An imbalance between intrahepatic lipid formation and secretion results in hepatic steatosis (19). In conditions where lipid balance is disrupted, inflammation, fibrosis, and even cancer may occur as damaged hepatocytes activate and cause hepatocyte regeneration (20). Conventional evaluation of the therapeutic efficacy of treatment for hepatic steatosis requires multiple liver biopsies, which have limitations such as invasiveness, sampling error, and interpretation variability (21).

MRI PDFF has the ability to help noninvasively quantify liver fat with high accuracy and reproducibility. We found a statistically significant genetic correlation between liver MRI PDFF and NAFLD (correlation coefficients, 0.74; $P < .001$). We also found that liver MRI PDFF showed a causal effect on the risk of NASH ($P < .001$) and NAFLD ($P < .001$). A decrease in liver MRI PDFF has shown predictive value for NAFLD activity

Table 4: Proportion of Effect Mediated for Exposure-Mediator-Outcome Relationships

Exposure	Mediator	Outcome	Proportion of Effect Mediated (%)	*P* Value
HDL-C	Liver MRI PDFF	NAFLD (K76.0)	25.1 (0, 56.7)	.046
T2DM	Liver MRI PDFF	NAFLD (K76.0)	46.3 (0, 92.8)	.008
Waist-to-hip ratio	Liver MRI PDFF	Fibrosis and cirrhosis of liver (K74)	37.0 (0, 79.0)	.003
Waist-to-hip ratio	Liver MRI PDFF	Cirrhosis of liver (K74.6)	28.7 (0.5, 56.9)	.004
Waist-to-hip ratio	Liver MRI PDFF	NAFLD (K76.0)	38.4 (0.4, 76.3)	.01

Note.—The codes in parentheses after the disease are defined from the 10th edition of the *International Classification of Diseases*. Data in parentheses are 95% CIs. HDL-C = high-density lipoprotein cholesterol, NAFLD = nonalcoholic fatty liver disease, PDFF = proton density fat fraction, T2DM = type 2 diabetes mellitus.

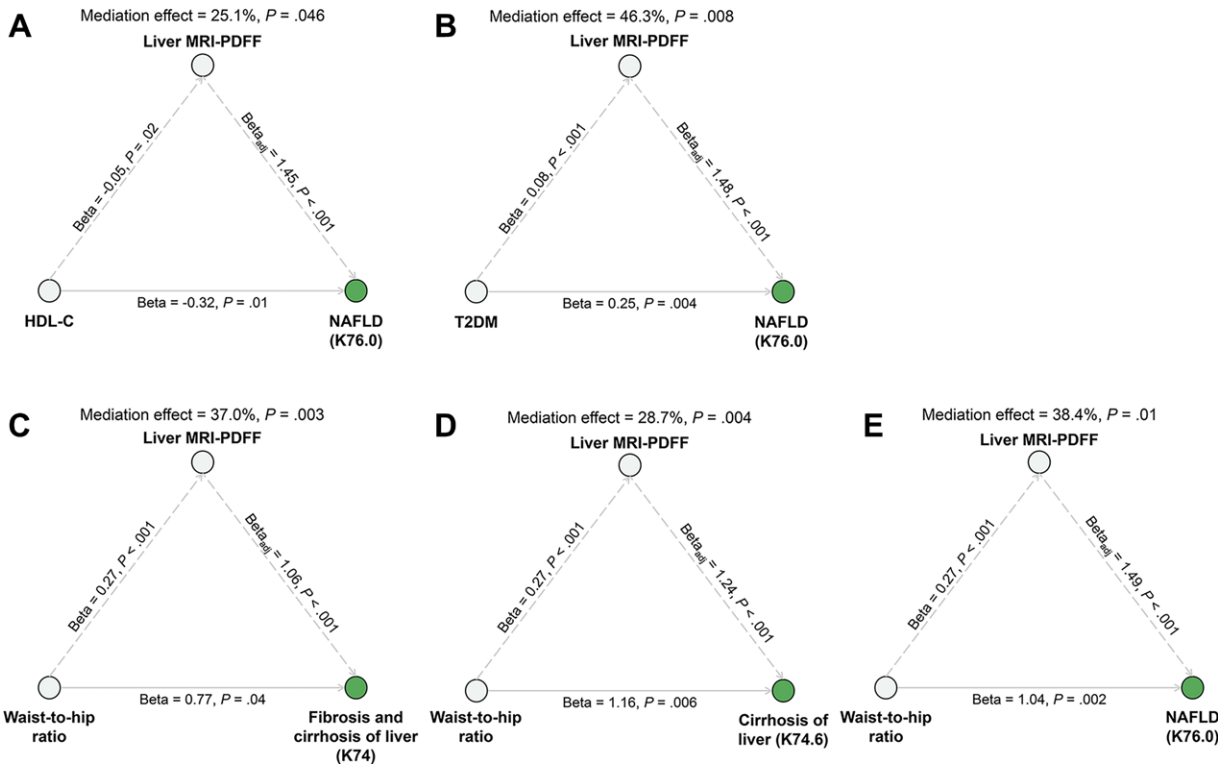

Figure 4: Mediation analysis of the effect of potential risk factors on liver diseases at liver MRI proton density fat fraction (PDFF). Analysis of the effect of **(A)** high-density lipoprotein cholesterol (HDL-C) and **(B)** type 2 diabetes mellitus (T2DM) on nonalcoholic fatty liver disease (NAFLD) as mediated at liver MRI PDFF. Analysis of the effect of waist-to-hip ratio on **(C)** fibrosis and cirrhosis of the liver, **(D)** cirrhosis of the liver, and **(E)** NAFLD as mediated at liver MRI PDFF, respectively. β and *P* values are calculated from univariable mendelian randomization (exposure outcome, exposure mediator) or multivariable (mediator outcome) mendelian randomization. The β value on the solid line represents the total effect and the product of the two β values on the dotted lines represents the indirect effect. The statistical significance of the mediation effect was tested by Sobel test. The codes in parentheses under the green dots are defined from the 10th edition of the *International Classification of Diseases*.

score response (6). It also demonstrated medium-high diagnostic performance for identifying NASH (22).

Our study showed a positive causal effect of liver MRI PDFF on the presence of fibrosis and cirrhosis of liver. A recent study (23) reported that PDFF had a higher performance in diagnosis of NASH with any fibrosis stage than MR elastography. Another study (24) showed that higher liver MRI PDFF was related to the progression of fibrosis in patients who had undergone liver biopsies. Notably, we obtained evidence that liver fat content accumulation may lead to fibrosis and even cirrhosis of the liver regardless of etiology.

We also found that liver MRI PDFF showed a causal effect on the risk of alcoholic liver disease ($P < .001$) and malignant liver neoplasm ($P < .001$). Excess fat accumulation is the earliest

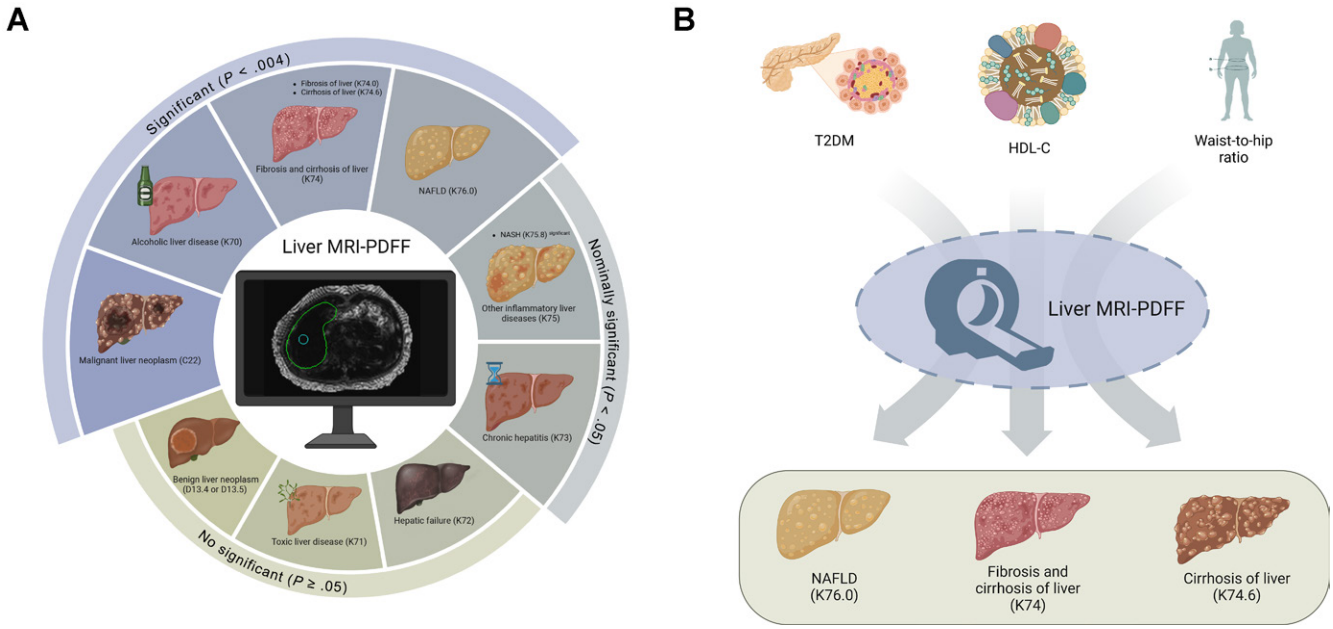

Figure 5: Summary concept diagrams show liver MRI proton density fat fraction (PDFF) causal association with liver disease and possible mediating role in the disease pathway. **(A)** The causal association between liver MRI PDFF and liver disease is shown. The phenotypes on the top left are significant, the phenotypes on the right are nominally significant, and the phenotypes on the bottom are not significant. **(B)** Liver MRI PDFF as a mediator to trigger indirect effects between phenotypes. Codes in parentheses are defined from the 10th edition of the *International Classification of Diseases*. HDL-C = high-density lipoprotein cholesterol, NAFLD = nonalcoholic fatty liver disease, NASH = nonalcoholic steatohepatitis, T2DM = type 2 diabetes mellitus.

and most typical hepatic reaction to alcohol, and hepatic steatosis commonly develops in alcohol-consuming individuals (25). Hepatocellular carcinoma, which is one of the most common liver malignancies and a leading cause of cancer-related mortality worldwide, has a predominance of NAFLD, NASH, and alcohol in European populations (26). Abnormal lipid metabolism promoting hepatocellular carcinoma is influenced by impaired immunologic function, pathologic inflammatory responses, and metabolic and oxidative stress specific to the liver (27).

Several major risk factors, including obesity, lipid metabolism, and type 2 diabetes mellitus, contribute to abnormal liver lipid metabolism (13). Our findings aligned with previous mendelian randomization studies that established causal associations between NAFLD risk and high-density lipoprotein cholesterol, type 2 diabetes mellitus, and waist-to-hip ratio (28,29). We further found that the risk effects of these factors on NAFLD risk were mediated through liver MRI PDFF, ranging from 25.1% to 46.3% (all $P < .05$). Additionally, the effects of waist-to-hip ratio on the risk of fibrosis and cirrhosis of the liver ($P = .003$) and cirrhosis of the liver ($P = .004$) were mediated through liver MRI PDFF with a mediation effect ranging from 28.7% to 37.0%. According to previous studies (30), adipose tissue generates the largest fatty acids found in liver triglycerides (59%) in people with NAFLD. Moreover, increased liver fat content was associated with an increased risk of liver fibrosis and cirrhosis (2).

Our mendelian randomization study addresses multiple important limitations of conventional observational studies. Nevertheless, our study also had several limitations. First, all data were from people of European ancestry. Therefore, the results of this study should be carefully generalized to other populations due to human genetic heterogeneity. Second, when implemented in clinical practice, the estimated effect needs to be treated with caution. Finally, the analysis was performed while assuming that liver MRI PDFF served as a mediator in our study. However, this assumption was reasonable because hepatic steatosis is the key point of occurrence of liver disease. Third, we were unable to completely rule out the possibility of unmeasured or unknown confounding factors that could influence the relationship between liver MRI PDFF and liver diseases. The number of SNPs was too few in each instrumental variable of liver disease to investigate the reverse causality.

In summary, our study included a comprehensive mendelian randomization analysis to infer the causal associations between liver MRI proton density fat fraction (PDFF) and liver health based on summary-level and individual-level data. We found evidence that liver MRI PDFF was a causal mediator between potential risk factors and several liver disease risks. Our study provides evidence that MRI PDFF has the potential to improve liver imaging–level prediction and interventions for liver health, which may have important implications in routine clinical practice.

Acknowledgements: The authors thank the UK Biobank, FinnGen, DIAbetes Genetics Replication and Meta-analysis (DIAGRAM), Global Lipids Genetics Consortium (GLGC), GIANT (Genetic Investigation of ANthropometric Traits), MAGIC (Meta-analyses of Glucose and Insulin-Related Traits Consortium), and other investigators' study for contributing to summary-level data in this study.

Author contributions: Guarantors of integrity of entire study, **T.X., M.D., H.L., J.Z., T.W., S.J.**; study concepts/study design or data acquisition or data analysis/interpretation, all authors; manuscript drafting or manuscript revision for important intellectual content, all authors; approval of final version of submitted manuscript, all authors; agrees to ensure any questions related to the work are appropriately resolved, all authors; literature research, **T.X., Y.W., T.W., S.J.**; clinical studies, **T.X., H.L., Y.W., J.Z., S.J.**; statistical analysis, **T.X., M.D., H.L., T.W.**; and manuscript editing, **T.X., M.D., H.L., S.J.**

Disclosures of conflicts of interest: **T.X.** No relevant relationships. **M.D.** No relevant relationships. **H.L.** No relevant relationships. **Y.W.** No relevant relationships. **J.Z.** No relevant relationships. **T.W.** No relevant relationships. **S.J.** No relevant relationships.

References

1. Chalasani N, Younossi Z, Lavine JE, et al. The diagnosis and management of nonalcoholic fatty liver disease: Practice guidance from the American Association for the Study of Liver Diseases. Hepatology 2018;67(1):328–357.
2. Powell EE, Wong VW, Rinella M. Non-alcoholic fatty liver disease. Lancet 2021;397(10290):2212–2224.
3. Baiceanu A, Mesdom P, Lagouge M, Foufelle F. Endoplasmic reticulum proteostasis in hepatic steatosis. Nat Rev Endocrinol 2016;12(12):710–722.
4. Tamaki N, Ajmera V, Loomba R. Non-invasive methods for imaging hepatic steatosis and their clinical importance in NAFLD. Nat Rev Endocrinol 2022;18(1):55–66.
5. Jayakumar S, Middleton MS, Lawitz EJ, et al. Longitudinal correlations between MRE, MRI PDFF, and liver histology in patients with nonalcoholic steatohepatitis: Analysis of data from a phase II trial of selonsertib. J Hepatol 2019;70(1):133–141.
6. Loomba R, Neuschwander-Tetri BA, Sanyal A, et al. Multicenter Validation of Association Between Decline in MRI PDFF and Histologic Response in NASH. Hepatology 2020;72(4):1219–1229.
7. Littlejohns TJ, Holliday J, Gibson LM, et al. The UK Biobank imaging enhancement of 100,000 participants: rationale, data collection, management and future directions. Nat Commun 2020;11(1):2624.
8. Wilman HR, Parisinos CA, Atabaki-Pasdar N, et al. Genetic studies of abdominal MRI data identify genes regulating hepcidin as major determinants of liver iron concentration. J Hepatol 2019;71(3):594–602.
9. Parisinos CA, Wilman HR, Thomas EL, et al. Genome-wide and Mendelian randomisation studies of liver MRI yield insights into the pathogenesis of steatohepatitis. J Hepatol 2020;73(2):241–251. [Published correction appears in J Hepatol 2020;73(6):1594–1595.]
10. Liu Y, Basty N, Whitcher B, et al. Genetic architecture of 11 organ traits derived from abdominal MRI using deep learning. eLife 2021;10:e65554.
11. Burgess S, Davey Smith G, Davies NM, et al. Guidelines for performing Mendelian randomization investigations: update for summer 2023. Wellcome Open Res 2023;4:186.
12. Martin S, Sorokin EP, Thomas EL, et al. Estimating the Effect of Liver and Pancreas Volume and Fat Content on Risk of Diabetes: A Mendelian Randomization Study. Diabetes Care 2022;45(2):460–468.
13. Stefan N, Häring HU, Cusi K. Non-alcoholic fatty liver disease: causes, diagnosis, cardiometabolic consequences, and treatment strategies. Lancet Diabetes Endocrinol 2019;7(4):313–324.
14. Kurki MI, Karjalainen J, Palta P, et al. FinnGen provides genetic insights from a well-phenotyped isolated population. Nature 2023;613(7944):508–518 [Published correction appears in Nature 2023;615(7952):E19.].
15. Skrivankova VW, Richmond RC, Woolf BAR, et al. Strengthening the reporting of observational studies in epidemiology using mendelian randomisation (STROBE-MR): explanation and elaboration. BMJ 2021;375:n2233.
16. Xin J, Jiang X, Ben S, et al. Association between circulating vitamin E and ten common cancers: evidence from large-scale Mendelian randomization analysis and a longitudinal cohort study. BMC Med 2022;20(1):168. [Published correction appears in BMC Med 2022;20(1):281.]
17. Song S, Jiang W, Zhang Y, Hou L, Zhao H. Leveraging LD eigenvalue regression to improve the estimation of SNP heritability and confounding inflation. Am J Hum Genet 2022;109(5):802–811.
18. Brion MJ, Shakhbazov K, Visscher PM. Calculating statistical power in Mendelian randomization studies. Int J Epidemiol 2013;42(5):1497–1501.
19. Cohen JC, Horton JD, Hobbs HH. Human fatty liver disease: old questions and new insights. Science 2011;332(6037):1519–1523.
20. Marra F, Svegliati-Baroni G. Lipotoxicity and the gut-liver axis in NASH pathogenesis. J Hepatol 2018;68(2):280–295.
21. Davison BA, Harrison SA, Cotter G, et al. Suboptimal reliability of liver biopsy evaluation has implications for randomized clinical trials. J Hepatol 2020;73(6):1322–1332.
22. Andersson A, Kelly M, Imajo K, et al. Clinical Utility of Magnetic Resonance Imaging Biomarkers for Identifying Nonalcoholic Steatohepatitis Patients at High Risk of Progression: A Multicenter Pooled Data and Meta-Analysis. Clin Gastroenterol Hepatol 2022;20(11):2451–2461.e3.
23. Li J, Lu X, Zhu Z, et al. Head-to-head comparison of magnetic resonance elastography-based liver stiffness, fat fraction, and T1 relaxation time in identifying at-risk NASH. Hepatology 2023. 10.1097/HEP.0000000000000417. Published online May 1, 2023.
24. Ajmera V, Park CC, Caussy C, et al. Magnetic Resonance Imaging Proton Density Fat Fraction Associates With Progression of Fibrosis in Patients With Nonalcoholic Fatty Liver Disease. Gastroenterology 2018;155(2):307–310.e2.
25. Jeon S, Carr R. Alcohol effects on hepatic lipid metabolism. J Lipid Res 2020;61(4):470–479.
26. Vogel A, Meyer T, Sapisochin G, Salem R, Saborowski A. Hepatocellular carcinoma. Lancet 2022;400(10360):1345–1362.
27. Anstee QM, Reeves HL, Kotsiliti E, Govaere O, Heikenwalder M. From NASH to HCC: current concepts and future challenges. Nat Rev Gastroenterol Hepatol 2019;16(7):411–428.
28. Xie J, Huang H, Liu Z, et al. The associations between modifiable risk factors and nonalcoholic fatty liver disease: A comprehensive Mendelian randomization study. Hepatology 2023;77(3):949–964.
29. Yuan S, Chen J, Li X, et al. Lifestyle and metabolic factors for nonalcoholic fatty liver disease: Mendelian randomization study. Eur J Epidemiol 2022;37(7):723–733.
30. Donnelly KL, Smith CI, Schwarzenberg SJ, Jessurun J, Boldt MD, Parks EJ. Sources of fatty acids stored in liver and secreted via lipoproteins in patients with nonalcoholic fatty liver disease. J Clin Invest 2005;115(5):1343–1351.

Radiology

COMMUNICATIONS • ERRATUM

Erratum for: Association between Liver MRI Proton Density Fat Fraction and Liver Disease Risk

Originally published in:

https://doi.org/10.1148/radiol.231007

Association between Liver MRI Proton Density Fat Fraction and Liver Disease Risk

Tianyi Xia, Mulong Du, Huiqin Li, Yuancheng Wang, Junhao Zha, Tong Wu, Shenghong Ju

Erratum in:

https://doi.org/10.1148/radiol.239027

In Figure 4C–E, **there were mistakes in the β values and they were changed (from left to right on the Fig, respectively) to 0.77, 1.16, and 1.04**.

This copy is for personal use only. To order copies, contact *reprints@rsna.org*